$BiInO_3$: A Polar Oxide with $GdFeO_3$-Type Perovskite Structure

Alexei A. Belik,*,† Sergey Yu. Stefanovich,‡ Bogdan I. Lazoryak,‡ and Eiji Takayama-Muromachi§

International Center for Young Scientists (ICYS) and Advanced Materials Laboratory (AML), National Institute for Materials Science (NIMS), 1-1 Namiki, Tsukuba, Ibaraki 305-0044, Japan, and Department of Chemistry, Moscow State University, Moscow, 119992, Russia

Received November 29, 2005. Revised Manuscript Received January 26, 2006

A new oxide, $BiInO_3$, was prepared using a high-pressure high-temperature technique at 6 GPa and 1273 K. $BiInO_3$ has the $GdFeO_3$-type perovskite structure, but crystallizes in the polar space group $Pna2_1$. Structure parameters of $BiInO_3$ were refined from laboratory X-ray powder diffraction data ($Z = 4$; $a =$ 5.95463(7) Å, $b = 5.60182(7)$ Å, and $c = 8.38631(11)$ Å). $BiInO_3$ shows a second-harmonic generation signal of about 120−140 times that of quartz. $BiInO_3$ decomposes at ambient pressure on heating above 873 K to give In_2O_3 and $Bi_{25}InO_{39}$. No phase transitions were found between 140 and 873 K using differential scanning calorimetry and differential thermal analysis. Vibrational properties of $BiInO_3$ were studied by Raman spectroscopy.

Introduction

Noncentrosymmetric compounds are of special interest in materials science because of their technologically important properties, such as ferroelectricity, piezoelectricity, pyroelectricity, and second-order nonlinear optical behavior, that is, frequency conversion or second-harmonic generation (SHG).[1] A number of strategies have been proposed to prepare noncentrosymmetric materials,[2−6] for example, utilizing cations with a lone pair of electrons, such as Bi^{3+} and Pb^{2+}.[2] Because of the stereochemically active lone pair, Bi^{3+} and Pb^{2+} usually have asymmetric coordination environments. The local acentricity is a necessary, but not sufficient condition for generating crystallographic noncentrosymmetry. A large group of materials that contain Bi^{3+} and Pb^{2+} do have crystallographic centrosymmetry. Nevertheless, this strategy has produced a number of interesting materials with a large spontaneous polarization[2,3,7−9] and is particularly of interest for preparation of new multiferroic materials,[2,3] where long-range orders of magnetic moments and electric dipoles coexist.

$BiMO_3$ has recently received a lot of attention as multiferroics[10−12] and in the investigation of solid solutions of $BiMO_3$−$PbTiO_3$ to improve ferroelectric properties of $PbTiO_3$, reduce the amount of lead, and find new morphotropic phase boundary piezoelectrics.[13−19] However, very little has been known so far experimentally about $BiMO_3$ with nonmagnetic ions (M = Al, Sc, Ga, and In)[19−22] in comparison to the extensively studied multiferroic $BiMnO_3$ and $BiFeO_3$.[23−26] In the course of our studies of $BiMO_3$ with

* To whom correspondence should be addressed. Tel.: +81 (029) 851-3354 (ext. 8587). Fax: +81 (029) 860-4706. E-mail: alexei.belik@nims.go.jp.
† ICYS.
‡ Moscow State University.
§ AML.

(1) Halasyamani, P. S.; Poeppelmeier, K. R. *Chem. Mater.* **1998**, *10*, 2753.
(2) Azuma, M.; Takata, K.; Saito, T.; Ishiwata, S.; Shimakawa, Y.; Takano, M. *J. Am. Chem. Soc.* **2005**, *127*, 8889.
(3) Hughes, H.; Allix, M. M. B.; Bridges, C. A.; Claridge, J. B.; Kuang, X.; Niu, H.; Taylor, S.; Song, W.; Rosseinsky, M. J. *J. Am. Chem. Soc.* **2005**, *127*, 13790.
(4) Welk, M. E.; Norquist, A. J.; Arnold, F. P.; Stern, C. L.; Poeppelmeier, K. R. *Inorg. Chem.* **2002**, *41*, 5119.
(5) Maggard, P. A.; Stern, C. L.; Poeppelmeier, K. R. *J. Am. Chem. Soc.* **2001**, *123*, 7742.
(6) Kepert, C. J.; Prior, T. J.; Rosseinsky, M. J. *J. Am. Chem. Soc.* **2000**, *122*, 5158.
(7) Belik, A. A.; Azuma, M.; Saito, T.; Shimakawa, Y.; Takano, M. *Chem. Mater.* **2005**, *17*, 269.
(8) Uratani, Y.; Shishidou, T.; Ishii, F.; Oguchi, T. *Jpn. J. Appl. Phys., Part 1* **2005**, *44*, 7130.
(9) Belik, A. A.; Iikubo, S.; Kodama, K.; Igawa, N.; Shamoto, S.; Niitaka, S.; Azuma, M.; Shimakawa, Y.; Takano, M.; Izumi, F.; Takayama-Muromachi, E. *Chem. Mater.* **2006**, *18*, 798.
(10) (a) Fiebig, M. *J. Phys. D: Appl. Phys.* **2005**, *38*, R123. (b) Prellier, W.; Singh, M. P.; Murugavel, P. *J. Phys.: Condens. Matter* **2005**, *17*, R803.
(11) Hill, N. A. *J. Phys. Chem. B* **2000**, *104*, 6694.
(12) Hill, N. A. *Annu. Rev. Mater. Res.* **2002**, *32*, 1.
(13) Inaguma, Y.; Miyaguchi, A.; Yoshida, M.; Katsumata, T.; Shimojo, Y.; Wang, R. P.; Sekiya, T. *J. Appl. Phys.* **2004**, *95*, 231.
(14) (a) Eitel, R. E.; Zhang, S. J.; Shrout, T. R.; Randall, C. A.; Levin, I. *J. Appl. Phys.* **2004**, *96*, 2828. (b) Cheng, J. R.; Meng, Z. Y.; Cross, L. E. *J. Appl. Phys.* **2005**, *98*, 084102.
(15) (a) Zhang, S. J.; Randall, C. A.; Shrout, T. R. *Appl. Phys. Lett.* **2003**, *83*, 3150. (b) Yoshimura, T.; Trolier-McKinstry, S. *Appl. Phys. Lett.* **2002**, *81*, 2065.
(16) Cheng, J. R.; Zhu, W. Y.; Li, N.; Cross, L. E. *Mater. Lett.* **2003**, *57*, 2090.
(17) Cheng, J.; Eitel, R.; Li, N.; Cross, L. E. *J. Appl. Phys.* **2003**, *94*, 605.
(18) Eitel, R. E.; Randall, C. A.; Shrout, T. R.; Rehrig, P. W.; Hackenberger, W.; Park, S. E. *Jpn. J. Appl. Phys., Part 1* **2001**, *40*, 5999.
(19) (a) Halilov, S. V.; Fornari, M.; Singh, D. J. *Phys. Rev. B* **2004**, *69*, 174107. (b) Iniguez, J.; Vanderbilt, D.; Bellaiche, L. *Phys. Rev. B* **2003**, *67*, 224107.
(20) Belik, A. A.; Wuernisha, T.; Kamiyama, T.; Mori, K.; Maie, M.; Nagai, T.; Matsui, Y.; Takayama-Muromachi, E. *Chem. Mater.* **2006**, *18*, 133.
(21) Baettig, P.; Schelle, C. F.; LeSar, R.; Waghmare, U. V.; Spaldin, N. A. *Chem. Mater.* **2005**, *17*, 1376.
(22) Belik, A. A.; Iikubo, S.; Kodama, K.; Igawa, N.; Shamoto, S.; Maie, M.; Nagai, T.; Matsui, Y.; Stefanovich, S. Yu.; Lazoryak, B. I.; Takayama-Muromachi, E. *J. Am. Chem. Soc.* **2006**, *128*, 706.
(23) Atou, T.; Chiba, H.; Ohoyama, K.; Yamaguchi, Y.; Syono, Y. *J. Solid State Chem.* **1999**, *145*, 639.
(24) Hill, N. A.; Rabe, K. M. *Phys. Rev. B* **1999**, *59*, 8759.
(25) Wang, J.; Neaton, J. B.; Zheng, H.; Nagarajan, V.; Ogale, S. B.; Liu, B.; Viehland, D.; Vaithyanathan, V.; Schlom, D. G.; Waghmare, U. V.; Spaldin, N. A.; Rabe, K. M.; Wuttig, M.; Ramesh, R. *Science* **2003**, *299*, 1719.

10.1021/cm052627s CCC: $33.50
Published on Web 03/01/2006

nonmagnetic M ions, we have shown that $BiGaO_3$ has a centrosymmetric pyroxene-type structure,[20] $BiScO_3$ has a centrosymmetric $BiMnO_3$-type perovskite structure,[22] and only $BiAlO_3$ crystallizes in a noncentrosymmetric structure and is isotypic with the well-known multiferroic $BiFeO_3$.[20]

In this work, we describe high-pressure synthesis, crystal structure, and characterization of a new perovskite-type oxide $BiInO_3$. The crystal structure of $BiInO_3$ was investigated by X-ray powder diffraction. $BiInO_3$ has the orthorhombic $GdFeO_3$-type distortion of the perovskite structure, but crystallizes in a polar space group. The thermal stability, Raman spectrum, and SHG efficiency of $BiInO_3$ are reported.

Experimental Section

Synthesis. A stoichiometric mixture of Bi_2O_3 and In_2O_3 (an amount of substance ratio of 1:1) was dried at 873 K for 8 h, then placed in Au capsules, and treated at 6 GPa in a belt-type high-pressure apparatus at 1273 K for 80 min. After heat treatment, the samples were quenched to room temperature (RT), and the pressure was slowly released. $BiInO_3$ was recovered from Au capsules as hard pellets, having light yellow color. According to X-ray powder diffraction (XRD), $BiInO_3$ contained a small amount of In_2O_3 and unidentified impurities. All of our attempts to prepare single-phased $BiInO_3$ by varying the synthesis conditions (temperature and time) failed. All of the samples contained some amount of impurities. Note that the kind and amount of impurities were different depending on the synthesis conditions.

Thermal Analysis. The thermal stability of $BiInO_3$ was examined on a SII Exstar 6000 (TG-DTA 6200) system at a heating rate of 10 K/min between RT and 1073 K. Differential scanning calorimetry (DSC) curves of $BiInO_3$ were recorded between 140 and 823 K at a heating rate of 5 K/min on a SII Exstar 6000 (DSC 6220) instrument in open aluminum capsules.

Vibrational Properties. Unpolarized Raman spectra of $BiInO_3$ were collected at RT with a micro Raman spectrometer (Horiba Jobin-Yvon T64000) in backscattering geometry with a liquid nitrogen cooled CCD detector. Raman scattering was excited using an Ar^+-Kr^+ laser at a wavelength of 514.5 nm. A 90× long working distance objective was used to focus the laser beam onto a spot of about 2 μm in diameter. The laser power on the $BiInO_3$ sample was about 0.2 mW. The surface of $BiInO_3$ was damaged by a larger laser power.

SHG Experiments. SHG responses of powder samples were measured in a reflection scheme. A Q-switch pulsed Nd:YAG laser operated at $\lambda_\omega = 1064$ nm was used as a radiation source with a repetition rate of 4 impulses/s and a duration of impulses of about 12 ns. The laser beam was split into two beams to excite the radiation at a doubled frequency, $\lambda_{2\omega}$, of 532 nm simultaneously in samples to be measured and a reference sample, polycrystalline α-SiO_2.

XRD Experiments and Structure Refinements. XRD data of $BiInO_3$ were collected at RT on a RIGAKU Ultima III diffractometer using Cu K_α radiation (2θ range of 18−150°, a step width of 0.02°, and a counting time of 9 s/step). The XRD data were analyzed by the Rietveld method with RIETAN-2000.[27] Coefficients for analytical approximation to atomic scattering factors for Bi, In, and O were taken from ref 28. The split pseudo-Voigt function of Toraya[29] was used as a profile function. The background was represented by a ninth-order Legendre polynomial. Isotropic atomic displacement parameters, U, with the isotropic Debye−Waller factor represented as $\exp(-8\pi^2 U \sin^2\theta/\lambda^2)$ were assigned to all of the sites. For the impurity of In_2O_3, we refined only a scale factor and the a lattice parameter, fixing its structure parameters. The mass percentage of In_2O_3 in $BiInO_3$ was calculated at 3.8% from the refined scale factors. 2θ regions containing reflections of unknown impurities were excluded from the refinement of $BiInO_3$.

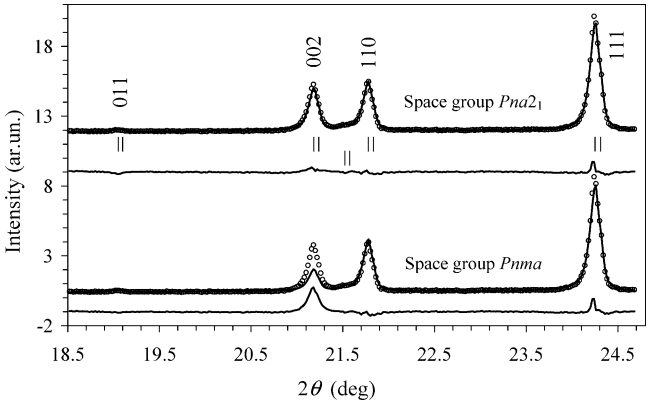

Figure 1. Fragments of the observed (○), calculated (−), and difference XRD patterns for $BiInO_3$ in the $Pna2_1$ and $Pnma$ models. Bragg reflections are indicated by tick marks. The lower tick marks are given for the impurity phase, In_2O_3. Indices of the reflections in $Pna2_1$ are given.

Results

Structure Refinement of $BiInO_3$ from XRD Data. Indexing Bragg reflections in the XRD pattern of $BiInO_3$ using TREOR[30] revealed it to crystallize in the orthorhombic system with lattice parameters of $a \approx 5.954$ Å, $b \approx 8.386$ Å, and $c \approx 5.602$ Å. Reflection conditions derived from the indexed reflections were $k + l = 2n$ for $0kl$, $h = 2n$ for $hk0$ and $h00$, $k = 2n$ for $0k0$, and $l = 2n$ for $00l$, affording possible space groups $Pnma$ (No. 62, centrosymmetric) and $Pn2_1a$ (No. 33, noncentrosymmetric).[31] The XRD pattern of $BiInO_3$ was found to be very similar to those of $GdFeO_3$-type compounds. Therefore, for initial fractional coordinates in Rietveld analysis of $BiInO_3$, we first used those of $CdTiO_3$ with space group $Pnma$.[32] However, the fit of some reflections (for example, (020) in $Pnma$, Figure 1) was bad, while in space group $Pn2_1a$, the fit of these reflections was considerably improved (Figure 1). The $Pnma$ model resulted in $R_{wp} = 12.78\%$ ($S = 3.45$), $R_p = 9.35\%$, $R_B = 7.72\%$, and $R_F = 3.93\%$, while the refinement in space group $Pn2_1a$ (standard setting: $Pna2_1$) gave noticeably lower R factors: $R_{wp} = 9.56\%$ ($S = 2.58$), $R_p = 7.30\%$, $R_B = 3.95\%$, and $R_F = 2.16\%$. In the $Pnma$ model, one U parameter for O was negative (−0.012(3) Å^2), and another was large (0.049(7) Å^2). It is known that disregarding a center of symmetry, if

(26) (a) Montanari, E.; Righi, L.; Calestani, G.; Migliori, A.; Gilioli, E.; Bolzoni, F. *Chem. Mater.* **2005**, *17*, 1765. (b) Montanari, E.; Calestani, G.; Migliori, A.; Dapiaggi, M.; Bolzoni, F.; Cabassi, R.; Gilioli, E. *Chem. Mater.* **2005**, *17*, 6457.
(27) Izumi, F.; Ikeda, T. *Mater. Sci. Forum* **2000**, *321−324*, 198.
(28) *International Tables for Crystallography*, 2nd ed.; Wilson, A. J. C., Prince, E., Eds.; Kluwer: Dordrecht, The Netherlands, 1999; Vol. C, pp 572−574.
(29) Toraya, H. *J. Appl. Crystallogr.* **1990**, *23*, 485.
(30) Werner, P. E.; Eriksson, L.; Westdahl, M. *J. Appl. Crystallogr.* **1985**, *18*, 367.
(31) *International Tables for Crystallography*, 5th ed.; Hahn, T., Ed.; Kluwer: Dordrecht, The Netherlands, 2002; Vol. A, p 52.
(32) Sasaki, S.; Prewitt, C. T.; Bass, J. D. *Acta Crystallogr., Sect. C* **1987**, *43*, 1668.

Table 1. Structure Parameters for $BiInO_3$[a]

site	Wyckoff position	x	y	z	10^2U (Å^2)
Bi	4a	0.05955(14)	0.0088(3)	0.7797(2)	0.91(3)
In[b]	4a	0.0026(4)	0.5011(14)	0	0.34(4)
O1	4a	−0.054(3)	0.383(3)	0.773(5)	0.7(4)
O2	4a	0.171(4)	0.218(4)	0.447(3)	2.3(8)
O3	4a	0.344(4)	0.630(3)	0.530(3)	0.2(6)

[a] Space group $Pna2_1$ (No. 33); $Z = 4$; $a = 5.95463(7)$ Å, $b = 5.60182(7)$ Å, $c = 8.38631(11)$ Å, and $V = 279.740(6)$ Å^3; $R_{wp} = 9.56\%$, $R_p = 7.30\%$, $R_B = 3.95\%$, $R_F = 2.16\%$, and $S = R_{wp}/R_e = 2.58$. Occupancy factors of all of the sites are unity. [b] The In site was placed at $z = 0$ due to the arbitrariness of setting the origin in the noncentrosymmetric space group of $Pna2_1$.

Table 2. Bond Lengths, l (Å), in $BiInO_3$

bonds	l	bonds	l
Bi−O1	2.20(1)	In−O2	1.93(2)
Bi−O3	2.28(2)	In−O1	2.05(4)
Bi−O2	2.34(3)	In−O3	2.21(2)
Bi−O1a	2.38(2)	In−O3a	2.28(2)
Bi−O3a	2.58(2)	In−O2a	2.34(2)
Bi−O2a	2.68(2)	In−O1a	2.40(4)
Bi−O2b	3.10(2)		

it is present, results in errors in the atomic coordinates that are large as compared to normal estimated standard deviations.[33] Both models gave the similar standard deviations for fractional atomic coordinates: $(2-4) \times 10^{-4}$ for Bi and $(2-3) \times 10^{-3}$ for O in space group *Pnma* and $(1-3) \times 10^{-4}$ for Bi and $(3-5) \times 10^{-3}$ for O in space group $Pna2_1$. All of these facts allowed us to conclude from the XRD data that $BiInO_3$ crystallizes in noncentrosymmetric space group $Pna2_1$.

The as-synthesized $BiInO_3$ and $BiInO_3$ heated to 823 K showed SHG signals of about 120−140 times that of α-quartz. The main phase was the same in these two samples, but impurities were different. Therefore, the SHG signal is believed to come from the main phase, proving that $BiInO_3$ crystallizes in the noncentrosymmetric space group.

Table 1 gives experimental and refinement conditions, lattice parameters, R factors, and so forth. Final fractional coordinates and U parameters in space group $Pna2_1$ for $BiInO_3$ are listed in Table 1, and selected bond lengths, l, calculated with ORFFE[34] are shown in Table 2. Figure 2 displays observed, calculated, and difference XRD patterns. Figure 3 shows the projections of the crystal structure of $BiInO_3$ along the b and c axes.

Thermal Stability of $BiInO_3$. The DTA curve showed an exothermic peak centered at about 920 K and an endothermic peak centered at 1020 K (see Supporting Information). XRD data collected after the heating of $BiInO_3$ up to 1073 K showed that $BiInO_3$ decomposed to a mixture of In_2O_3 and $Bi_{25}InO_{39}$. The same mixture (In_2O_3 and $Bi_{25}InO_{39}$) was obtained by heating In_2O_3 and Bi_2O_3 at 1023 K and ambient pressure for 10 h. The endothermic peak at 1020 K was proved to be originated from the mixture of In_2O_3 and $Bi_{25}InO_{39}$. The exothermic peak at 920 K corresponds to the decomposition of $BiInO_3$ that starts from about 873 K.

(33) Marsh, R. E. *Acta Crystallogr., Sect. B* **1995**, *51*, 897.
(34) Busing, W. R.; Martin, K. O.; Levy H. A. *Report ORNL-TM-306*; Oak Ridge National Laboratory: TN, 1964.

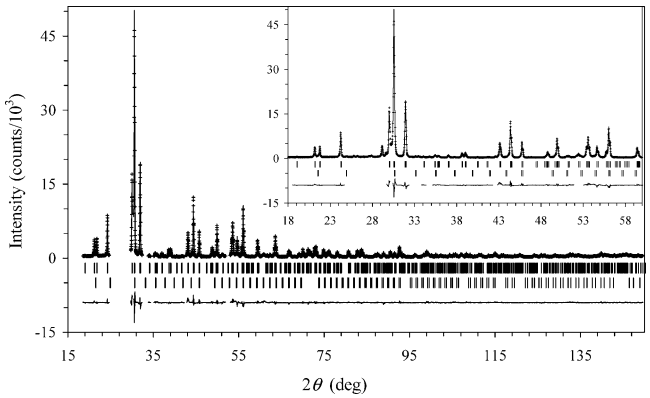

Figure 2. Observed (+) and calculated (−) XRD patterns for $BiInO_3$ in the $Pna2_1$ model. The difference pattern is shown at the bottom. The missing parts on the XRD patterns give the regions excluded from the refinement. Bragg reflections are indicated by tick marks. The lower tick marks are given for the impurity phase, In_2O_3. Inset shows the enlarged fragment with the full observed XRD pattern.

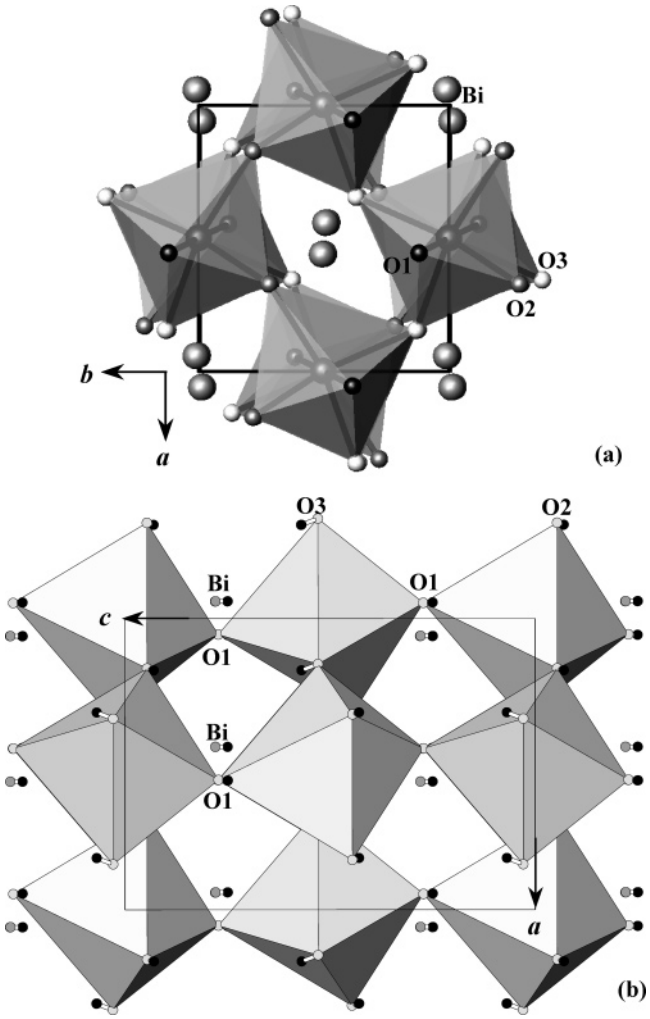

Figure 3. (a) Schematic projection view of the structure of $BiInO_3$ along the c axis. The InO_6 octahedra are drawn. The Bi atoms are shown by circles. (b) Schematic projection view of the structure of $BiInO_3$ along the b axis. The InO_6 octahedra are drawn. Black circles show the positions of atoms in a hypothetical *Pnma* structure.

The DSC curve from 140 to 823 K showed one very broad anomaly near 623 K. The same anomaly was observed in $BiAlO_3$, $BiGaO_3$, and $BiScO_3$.[20] Its origin seems to be annealing effects. The above data indicate that no structural

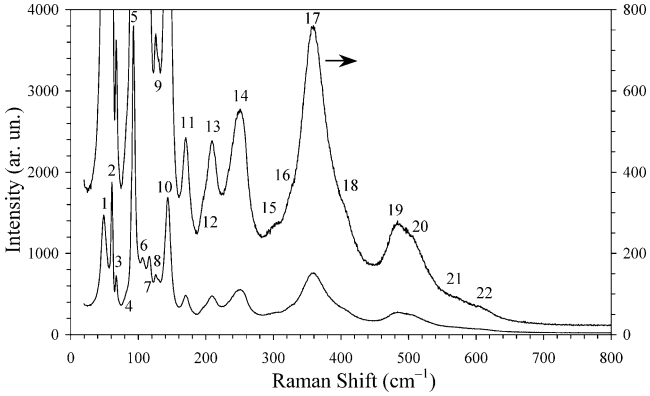

Figure 4. Raman spectrum of $BiInO_3$ at room temperature. The enlarged Raman spectrum is present using the secondary axis. Numbers count the observed Raman bands.

phase transitions occur in $BiInO_3$ below 873 K down to 140 K.

Raman Spectroscopy of $BiInO_3$. $BiInO_3$ (space group C_{2v}^9) has four formula units in the primitive cell and 60 degrees of vibrational freedom. Factor group analysis[35] predicts the following modes: $14A_1 + 15A_2 + 14B_1 + 14B_2$. Because all of the modes are Raman active, 57 Raman modes are expected. Factor group analysis for the *Pnma* (D_{2h}^{16}) model predicts the following modes: $7A_g + 5B_{1g} + 7B_{2g} + 5B_{3g} + 8A_u + 10B_{1u} + 8B_{2u} + 10B_{3u}$. Raman active modes are A_g, B_{1g}, B_{2g}, and B_{3g}. Therefore, maximum 24 Raman modes ($7A_g + 5B_{1g} + 7B_{2g} + 5B_{3g}$) should be present if the space group of $BiInO_3$ were *Pnma*. We observed 22 Raman modes experimentally (Figure 4).

Discussion

There are a large number of perovskite-type compounds that crystallize in the orthorhombically distorted $GdFeO_3$-type structure with $a \approx \sqrt{2}a_p$, $b \approx 2a_p$, and $c \approx \sqrt{2}a_p$, where $a_p \approx 3.8$ Å is the parameter of the cubic perovskite subcell. The overwhelming majority of the $GdFeO_3$-type compounds have centrosymmetric crystal structure with space group *Pnma*. In the middle of the last century, some of the $GdFeO_3$-type compounds were described as noncentrosymmetric, for example, $CdTiO_3$ and $LaYbO_3$.[32,36] However, their structures were revised latter using more advanced diffraction techniques and other methods (SHG and piezoelectric tests), and they were shown to be centrosymmetric belonging to space group *Pnma*.[32,36] Sometimes it is very difficult to distinguish between space groups *Pnma* and $Pna2_1$ using diffraction methods or Raman spectroscopy, for example, in $CdTiO_3$.[37] Only the observation of ferroelectric properties below a certain temperature (77 K in $CdTiO_3$) allowed for the conclusion that a centrosymmetric−noncentrosymmetric phase transition occurs.[37]

In the case of $BiInO_3$, the powder diffraction data allowed us to unambiguously distinguish between space groups *Pnma* and $Pna2_1$. This is attributed to a large structure distortion of $BiInO_3$, that is, a large displacement (~0.25 Å) of heavy Bi^{3+} ions from the mirror plane of *Pnma*. The space group $Pna2_1$ is polar and allows a spontaneous polarization. The polarization of $BiInO_3$ was calculated using the point charge model:

$$P_s = \sum_i Q_i z_i / V \qquad (1)$$

where Q_i is the formal ionic charge of each atom, z_i is its displacement along the *c* axis in $Pna2_1$ with respect to a hypothetical unpolarized *Pnma* structure (see Supporting Information), and *V* is the unit cell volume. This formula gives $P_s = 18\ \mu C/cm^2$.

Because $BiInO_3$ crystallizes in the polar structure at RT, one may expect that a polar−nonpolar phase transition should take place at higher temperatures. However, we could not detect any phase transitions in $BiInO_3$ with the DSC and DTA measurements up to the decomposition temperature of 873 K. Therefore, the Curie temperature of $BiInO_3$ at ambient pressure seems to be higher than 873 K.

Bi^{3+} ions are located in a strongly distorted oxygen environment (Table 2 and Figure 3). Four Bi−O distances are short (2.20−2.38 Å), and the other three Bi−O distances are long (2.58−3.10 Å). Therefore, the lone electron pair of a Bi^{3+} ion is active in $BiInO_3$, resulting in the parallel cooperative displacements of Bi^{3+} ions in the *c* direction away from the centroids of their oxygen coordination environments (Figure 3b). Note that $LaInO_3$ containing no stereochemically active ions crystallizes in space group *Pnma* with La lying on the mirror plane.[38] To obtain information on formal oxidation states of Bi and In, we calculated the bond valence sums, BVS,[39] of the Bi and In sites in $BiInO_3$ from the Bi−O and In−O bond lengths. The resulting BVS values were 2.87 for Bi and 2.97 for In. These BVS values support the oxidation state of +3 for Bi and In.

The average tilting angle, $\langle\omega\rangle$, of the InO_6 octahedra was determined from the θ_1(In−O1−In) = 141.3°, θ_2(In−O2−In) = 145.3°, and θ_3(In−O3−In) = 131.8° superexchange angles with the equations:[40]

$$\langle\omega\rangle = (180 - \langle\theta\rangle)/2$$

and

$$\langle\theta\rangle = (\theta_1 + \theta_2 + \theta_3)/3 \qquad (2)$$

These equations give $\langle\omega\rangle = 20.3°$. The $\langle\omega\rangle$ and θ_i values indicate that the titling is rather large. Similar θ_i values were observed in $BiNiO_3$, which crystallizes in triclinically distorted $GdFeO_3$-type structure (space group $P\bar{1}$).[41] Because of the large titling of the InO_6 octahedra, the coordination

(35) Rousseau, D. L.; Bauman, R. P.; Porto, S. P. S. *J. Raman Spectrosc.* **1981**, *10*, 253.
(36) Moreira, R. L.; Feteira, A.; Dias, A. *J. Phys.: Condens. Matter* **2005**, *17*, 2775.
(37) (a) Shan, Y. J.; Mori, H.; Tezuka, K.; Imoto, H.; Itoh, M. *Ferroelectrics* **2003**, *284*, 281. (b) Sun, P. H.; Nakamura, T.; Shan, Y. J.; Inaguma, Y.; Itoh, M. *Ferroelectrics* **1998**, *217*, 137.
(38) Park, H. M.; Lee, H. J.; Park, S. H.; Yoo, H. I. *Acta Crystallogr., Sect. C* **2003**, *59*, 131.
(39) Brese, R. E.; O'Keeffe, M. *Acta Crystallogr., Sect. B* **1991**, *47*, 192.
(40) See, for example: Pinsard-Gaudart, L.; Rodriguez-Carvajal, J.; Daoud-Aladine, A.; Goncharenko, I.; Medarde, M.; Smith, R. L.; Revcolevschi, A. *Phys. Rev. B* **2001**, *64*, 064426.
(41) Ishiwata, S.; Azuma, M.; Takano, M.; Nishibori, E.; Takata, M.; Sakata, M.; Kato, K. *J. Mater. Chem.* **2002**, *12*, 3733.

number of a large cation changed from 12 in an ideal cubic perovskite to 6+1 in $BiInO_3$.

The stability and distortions of perovskite-type oxides can be qualified using the tolerance factor, t:

$$t = \frac{r_A + r_O}{\sqrt{2}(r_B + r_O)} \quad (3)$$

where r_A, r_B, and r_O are the ionic radii of the A, B, and oxygen ions, respectively, in perovskite ABO_3. We used the r values for six-fold coordination, $r_{Bi} = 1.03$ Å, $r_{In} = 0.80$ Å, and $r_O = 1.40$ Å.[42] In this case (that is, r for 6-fold coordination), the stability of the perovskite structure is expected within the limits $0.77 < t < 0.99$.[18] Therefore, $BiInO_3$ with $t = 0.78$ is located just near the stability region.

The number of the observed Raman bands in $BiInO_3$ was smaller than the predicted number for the *Pnma* and $Pna2_1$ models. Therefore, we could not distinguish unambiguously between *Pnma* and $Pna2_1$ using Raman spectroscopy. However, the number of the observed Raman bands in the $GdFeO_3$-type compounds belonging to space group *Pnma* is usually about 2 times smaller than the predicted number of 24, for example, 8 in $CaFeO_3$,[43] 12 in $LaYbO_3$,[36] and 12 in $LaMnO_3$.[44] The polarized Raman measurements using single crystals allow one to detect more Raman bands, for example, 19 in $YMnO_3$.[44] The observation of 22 Raman modes in the powder $BiInO_3$ sample gives indirect evidence about the correct space group.

In conclusion, we prepared a new oxide $BiInO_3$ that crystallizes in a polar $GdFeO_3$-type perovskite structure. Structure parameters of $BiInO_3$ were refined from X-ray powder diffraction data. Thermal stability, vibrational properties, and second-harmonic generation efficiency of $BiInO_3$ were studied.

Acknowledgment. ICYS is supported by Special Coordination Funds for Promoting Science and Technology from MEXT, Japan.

Supporting Information Available: DSC and DTA curves of $BiInO_3$ (Figure S1); O−In−O bond angles (Table S1); structure parameters of $BiInO_3$ determined in space group *Pnma* (Table S2) (PDF). This material is available free of charge via the Internet at http://pubs.acs.org.

CM052627S

(42) Shannon, R. D. *Acta Crystallogr., Sect. A* **1976**, *32*, 751.

(43) Ghosh, S.; Kamaraju, N.; Seto, M.; Fujimori, A.; Takeda, Y.; Ishiwata, S.; Kawasaki, S.; Azuma, M.; Takano, M.; Sood, A. K. *Phys. Rev. B* **2005**, *71*, 245110.

(44) Iliev, M. N.; Abrashev, M. V.; Lee, H. G.; Popov, V. N.; Sun, Y. Y.; Thomsen, C.; Meng, R. L.; Chu, C. W. *Phys. Rev. B* **1998**, *57*, 2872.